ELECTRONIC SUPPLEMENTARY INFORMATION

Performance of ionomer blend-nanocomposite as an effective gas barrier material for organic devices

Sindhu Seethamraju,[a] Praveen C. Ramamurthy[*a,b] and Giridhar Madras[a]

[a]*Centre for Nanoscience and Engineering, Indian Institute of Science, Bangalore, 560012, India.*

[b]*Department of Materials Engineering, Indian Institute of Science, Bangalore, 560012, India.*

[*] Corresponding author: Phone:91-80-22932627; Email:onegroupb203@gmail.com

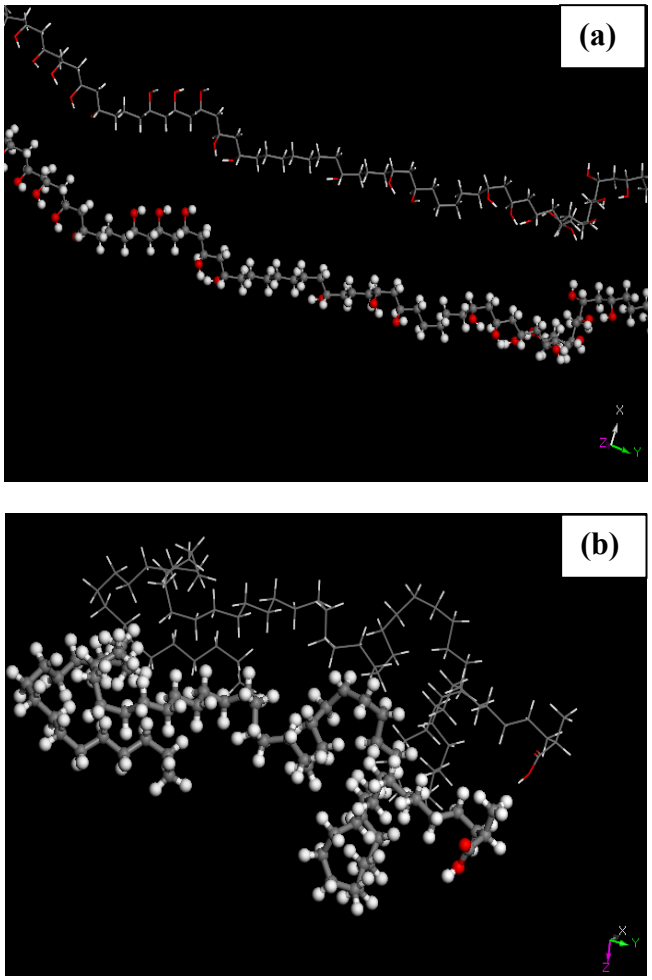

Figure S1. Atomistic representation of polymeric chains of **(a)** EVOH and **(b)** PEMA (with hydrogen, carbon and oxygen in white, grey and red colors respectively).

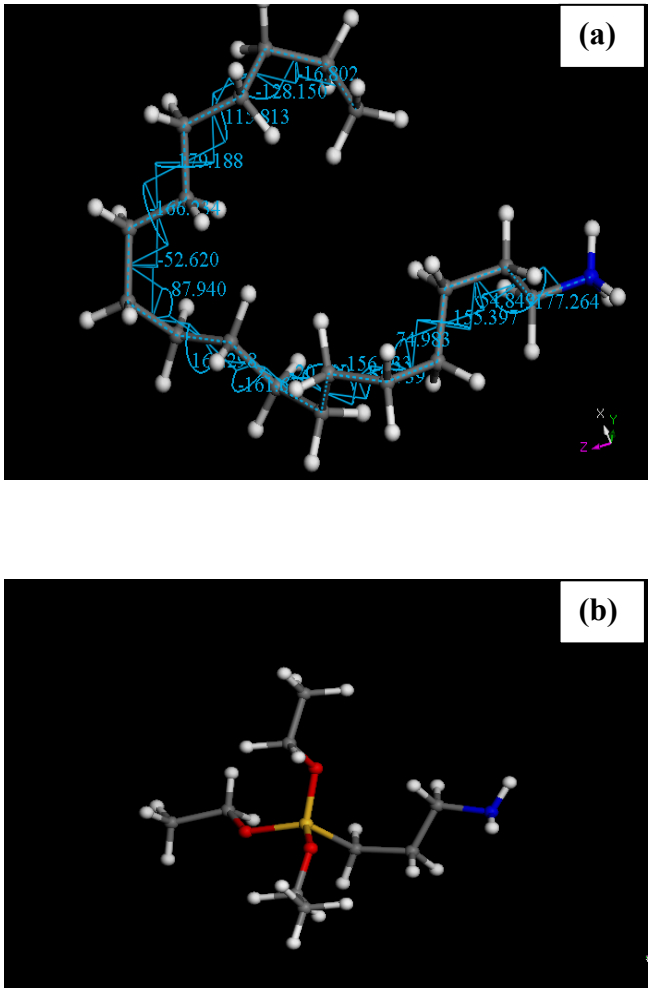

Figure S2. Representation of **(a)** ODA conformer and **(b)** APTMS (with hydrogen, carbon, oxygen, nitrogen and silicon in white, grey, red, blue and yellow color respectively).

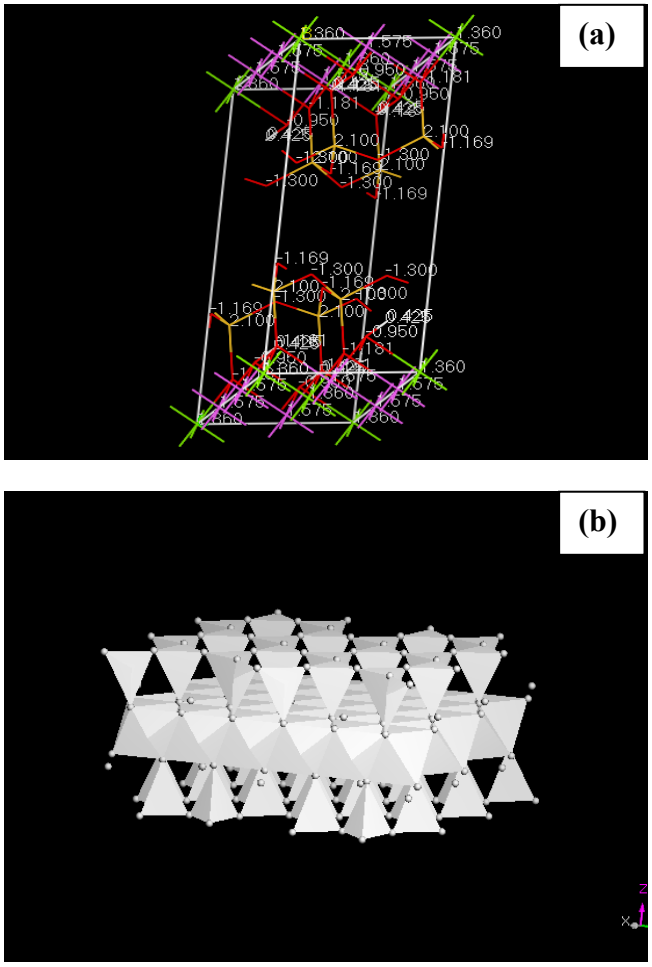

Figure S3. Montmorillonite clay **(a)** in crystal lattice with charging **(b)** platelet structure with octahedral alumina sandwiched between tetrahedral silicates with basal surface area of 20Å x 20Å.

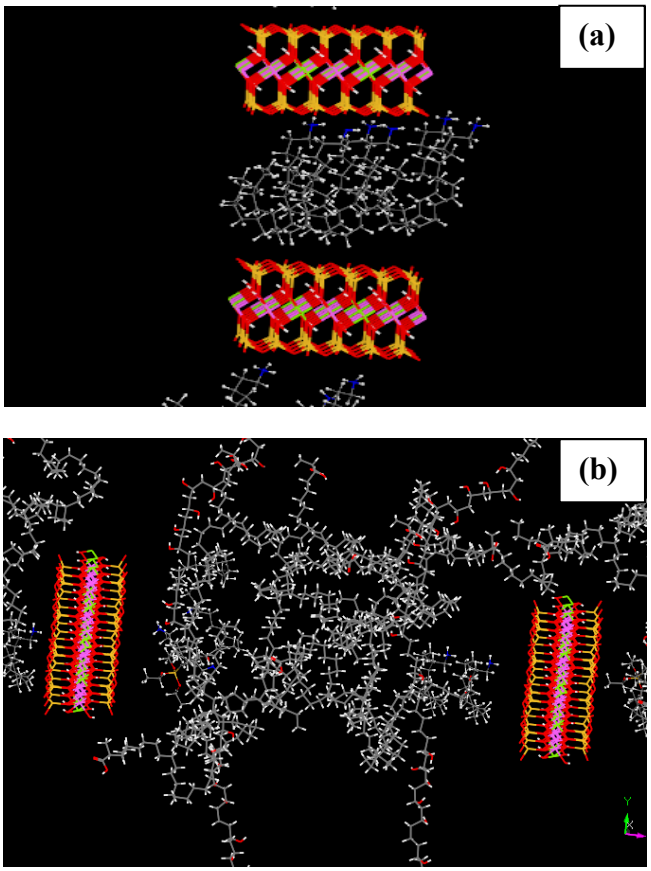

Figure S4. (a) Modified montmorillonite (MMT) clay with ODA and APTMS in the gallery spacing **(b)** PEMA/EVOH/MMT composite system after MDSA dynamics.

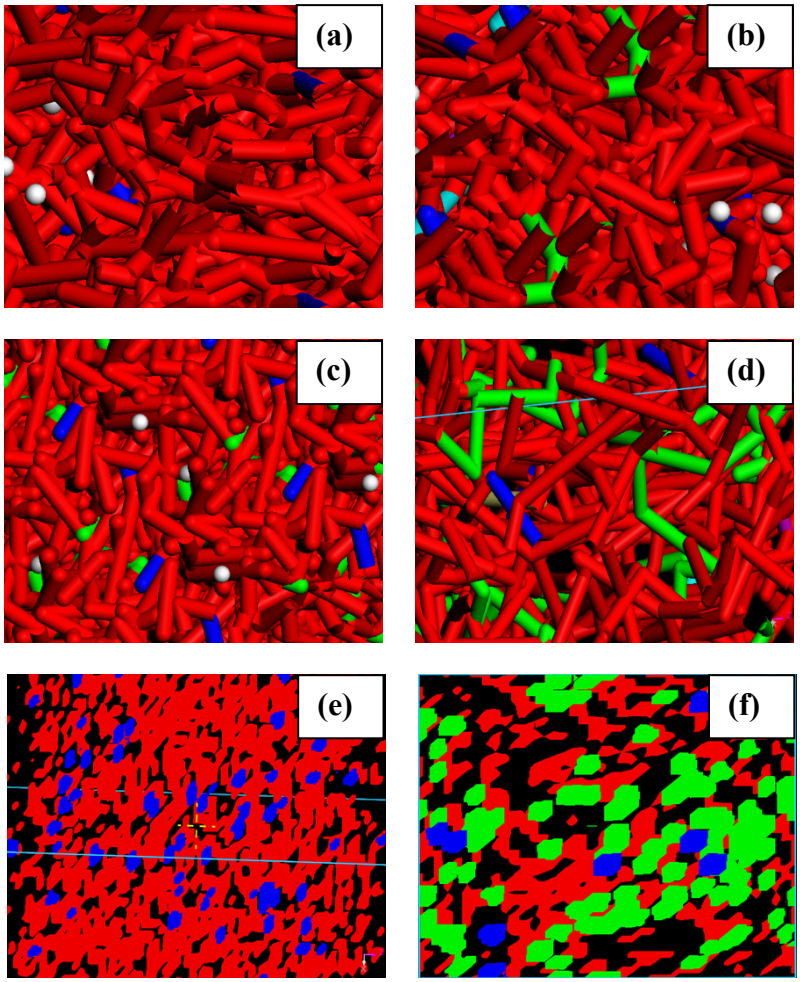

Figure S5. DPD unit system with the beads of PEMA (P1 (in blue), E1 (in red)), EVOH (E1 (in red), E2 (in green)), H2O (in grey) and O2 (in white) in the blend systems **(a)** B00 **(b)** B10 **(c)** B20 **(d)** B30 and sliced unit DPD cells for E1, E2 and P1 densities in **(e)** B00 and **(f)** B30 compositions.

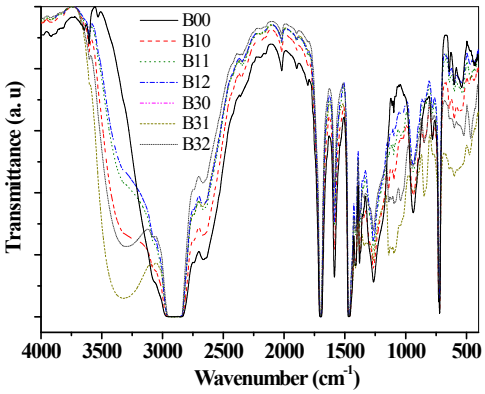

Figure S6. FTIR analysis for the blend compositions B00, B10, B30, B11, B12, B31 and B32.

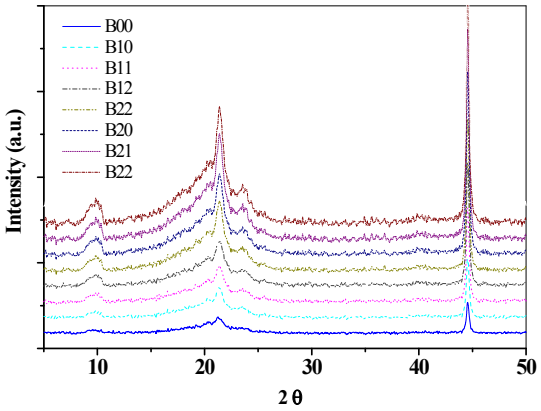

Figure S7. XRD analysis for the blend composites from 10° to 50°.

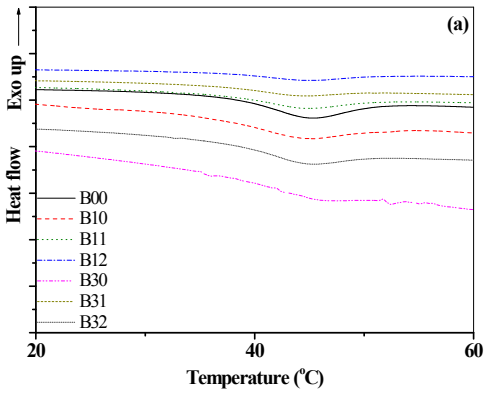
(a)
Exo up
Heat flow
B00
B10
B11
B12
B30
B31
B32
20
40
60
Temperature (°C)

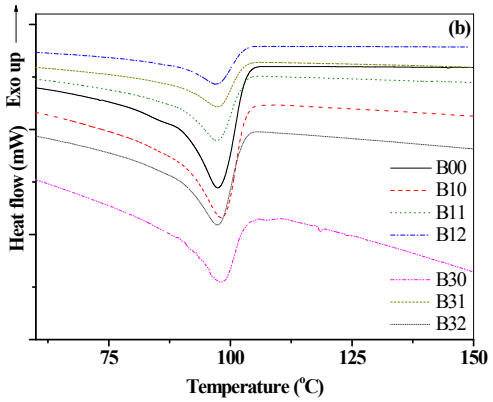
(b)
Exo up
Heat flow (mW)
B00
B10
B11
B12
B30
B31
B32
75
100
125
150
Temperature (°C)

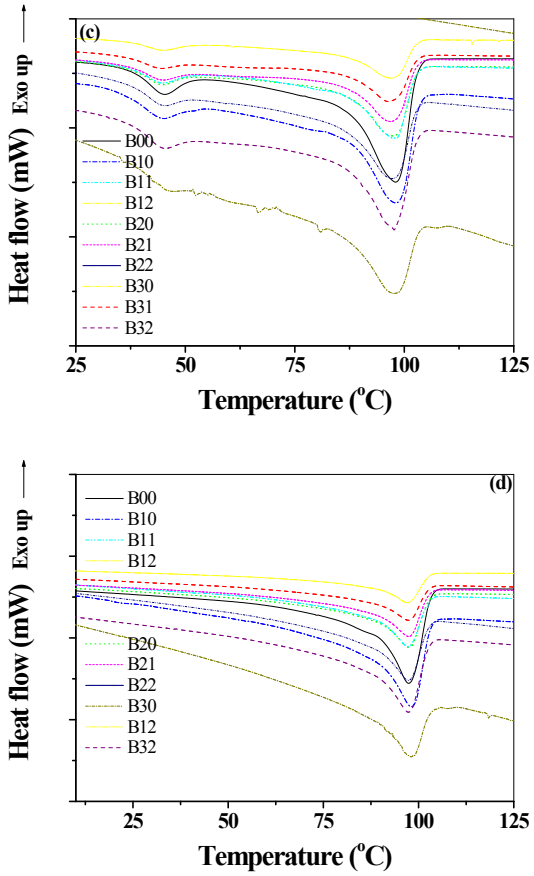

Figure S8. DSC analysis for the blend compositions B00, B10, B30, B11, B12, B31 and B32 **(a)** for order-disorder transitions **(b)** for melting properties **(c)** First heating cycle and **(d)** second heating cycle for all the films.

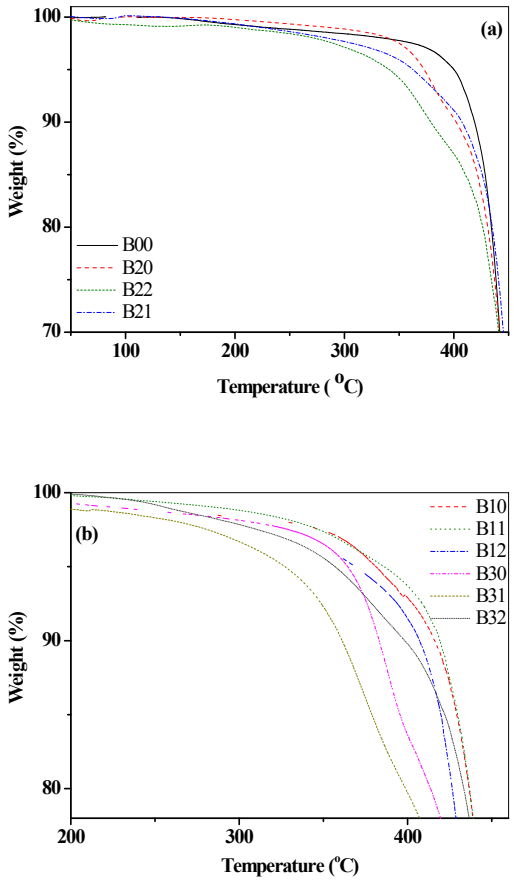

Figure S9. Thermogravimetric analysis for the neat surlyn, **(a)** B2 series blend and **(b)** B1 and B3 series.

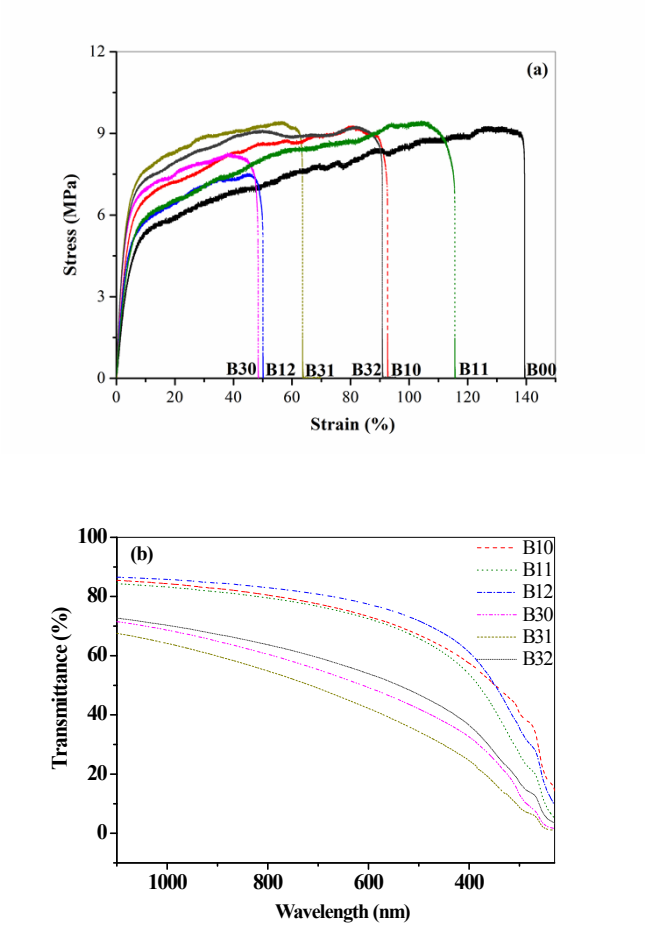

Figure S10. (a) Tensile analysis and **(b)** UV-visible transparency for the blend compositions B00, B10, B30, B11, B12, B31 and B32.

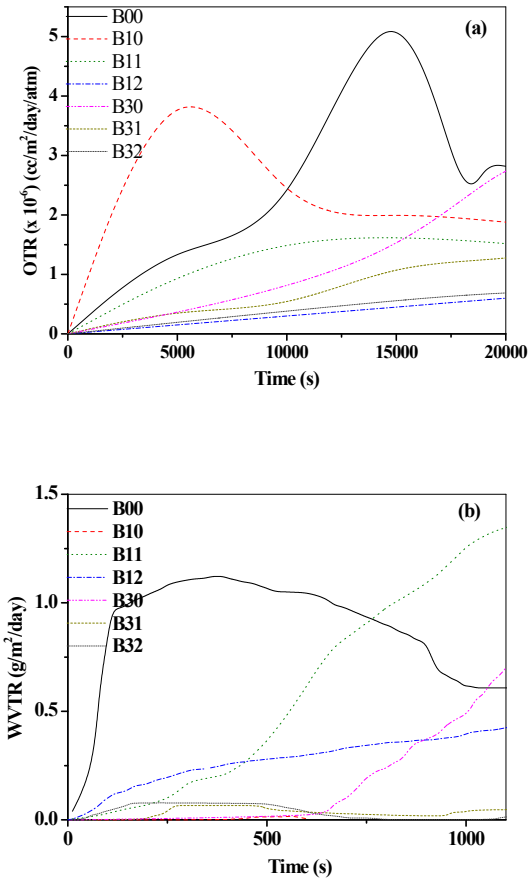

Figure S11. (a) OTR from calcium degradation tests **(b)** WVTR from CRDS based permeability setup for the blend compositions B10, B30, B11, B12, B31 and B32.

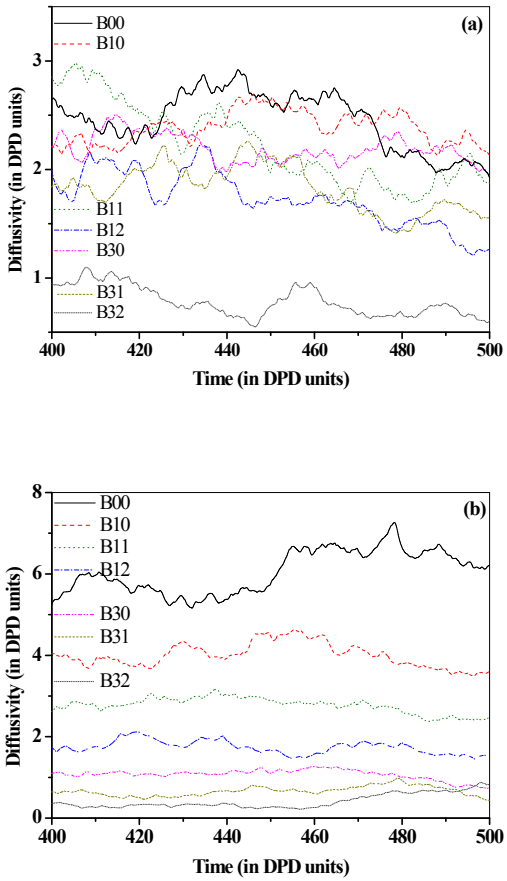

Figure S12. Diffusivities of **(a)** O2 and **(b)** H2O beads through the neat, blend and composite films (B00, B10, B11, B12, B30, B31 and B32), over the 400-500 DPD time units from the scaled DPD simulations.

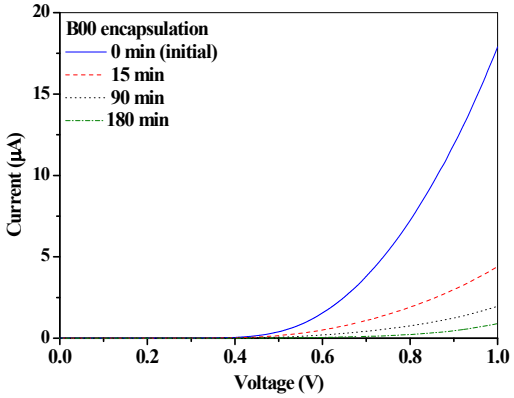

Figure S13. J-V Characteristics for encapsulated P3HT based Schottky device with B00 film before and after accelerated aging at different times.